MODELLING THE INNOVATION:
Communications, Automation and Information Systems
M. Carnevale, M. Lucertini and S. Nicosia (Editors)
Elsevier Science Publishers B.V. (North-Holland)
© IFIP, 1990

Dynamic Modelling of Multi-Link Flexible Robot Arms

Alessandro De Luca

Dipartimento di Informatica e Sistemistica
Università degli Studi di Roma "La Sapienza"
Via Eudossiana 18, 00184 Roma, Italy

Bruno Siciliano

Dipartimento di Informatica e Sistemistica
Università degli Studi di Napoli "Federico II"
Via Claudio 21, 80125 Napoli, Italy

The closed-form dynamic model of a planar multi-link flexible arm is derived based on a Lagrangian/assumed modes technique. A case study is developed for a two-link arm.

1. INTRODUCTION

One of the significant trends in today's robotics design is the adoption of fast, dexterous, lightweight mechanical structures to replace slow, conventional, massive industrial robot manipulators. Increasing the typically low payload-to-arm weight ratio is a promising engineering goal, and may prove very useful in non-standard applications such as space telerobotics.

In order to fully exploit the potential advantages offered by lightweight robot arms, one must explicitly consider the effects of the structural link flexibility and properly deal with (active and/or passive) control of vibrational behaviour. For simulation and control purposes, the need for an accurate dynamic model of a flexible manipulator is even more relevant than in the case of a rigid manipulator.

Many techniques exist in the literature for modelling open serial kinematic chains containing one or more flexible members. Just as in the case of rigid links, Newton-Euler and Lagrange-Euler formulations are typically adopted on the basis of a suitable kinematic description of both rigid and deflected motions. The former is recursive in nature and thus computationally advantageous, but the latter is usually preferred since it yields closed-form expressions of all dynamic terms [1].

As for the inherently distributed character of the flexible part of the system, finite-dimensional models are often used which approximate the "true" infinite-dimensional models [2]. In any case, link elasticity is usually modelled as a *linear* effect. The most currently used approximate descriptions of the deflection are based on assumed modes [3], finite elements [4], or Ritz-Kantorovich expansions [5], with different implications on the model complexity.

On one hand, *explicit* models have been derived for one-link flexible arms [3,6,7]. In this regard, it can be said that the one-link case is now well understood, but its simplicity prevents from thoroughly understanding the full nonlinear interactions between rigid and flexible components of arm dynamics.

On the other hand, for automatic generation of models for multi-link arms symbolic manipulation languages have been employed, e.g. MACSYMA [5,8]. Besides, a number of

numerical software packages are available for simulation purposes, but their intrinsic limitation is that the resulting model is only *implicitly* specified. In any case, the control engineer is offered poor insight into the origin of the single dynamic terms.

The aim of this work is to outline the basic steps for developing dynamic models of multi-link flexible robot arms. We will limit ourselves to the case of a planar multi-link flexible arm with no torsional effects. In this framework are also the works reported in [9,10] for a one-rigid/one-flexible link arm.

In particular, a closed-form symbolic dynamic model is derived for a two-link arm with two assumed modes of bending deformation for each link, using a Lagrangian technique. Links are modelled as Euler-Bernoulli beams of uniform density. A payload is added at the tip of the outer link, while hub inertias are included at the actuated joints. The implications of using proper mode shapes of deformation with clamped-mass boundary conditions are discussed. A set of simulation results are provided to validate the overall modelling.

It is argued that the considered case study is general enough to provide a basis for studying more complex structures, since most of the possible dynamic interaction effects are present.

2. KINEMATIC MODELLING

Consider a planar n-link flexible arm with rotary joints subject only to bending deformations in the plane of motion (torsional effects are neglected); Fig. 1 shows a two-link example. According to [1], the following coordinate frames are established: the inertial frame $(\widehat{X}_0, \widehat{Y}_0)$, the rigid body moving frame associated to link i (X_i, Y_i), and the flexible body moving frame associated to link i $(\widehat{X}_i, \widehat{Y}_i)$. The rigid motion is described by the joint angles θ_i, while $y_i(x_i)$ denotes the lateral deflection of link i at abscissa x_i, $0 \leq x_i \leq \ell_i$, being ℓ_i the link length.

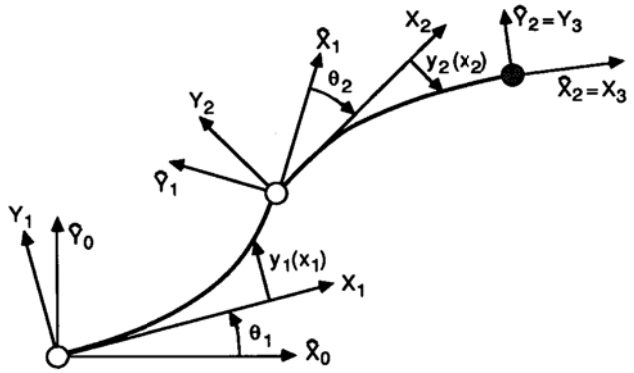

Fig. 1 — Schematic of a planar two-link flexible arm

Let then ${}^i\mathbf{p}_i(x_i) = (x_i \quad y_i(x_i))^T$ be the position of a point along the deflected link i with respect to frame (X_i, Y_i) and $\mathbf{p}_i$ be the absolute position of the same point in frame $(\widehat{X}_0, \widehat{Y}_0)$. Also, ${}^i\mathbf{r}_{i+1} = {}^i\mathbf{p}_i(\ell_i)$ indicates the position of the origin of frame (X_{i+1}, Y_{i+1}) with respect to frame (X_i, Y_i), and $\mathbf{r}_i$ its absolute position in frame $(\widehat{X}_0, \widehat{Y}_0)$.

The joint (rigid) rotation matrix $\mathbf{A}_i$ and the rotation matrix $\mathbf{E}_i$ of the (flexible) link at the end-point are, respectively,

$$\mathbf{A}_i = \begin{bmatrix} \cos\theta_i & -\sin\theta_i \\ \sin\theta_i & \cos\theta_i \end{bmatrix}, \qquad \mathbf{E}_i = \begin{bmatrix} 1 & -y'_{ie} \\ y'_{ie} & 1 \end{bmatrix} \tag{1}$$

where $y'_{ie} = (\partial y_i/\partial x_i)|_{x_i=\ell_i}$, and the linear approximation $\arctan y'_{ie} \simeq y'_{ie}$ valid for small deflections has been made. This also implies that all second-order terms involving products of deformations are neglected. Therefore, the above absolute position vectors can be expressed as

$$\mathbf{p}_i = \mathbf{r}_i + \mathbf{W}_i{}^i\mathbf{p}_i, \qquad \mathbf{r}_{i+1} = \mathbf{r}_i + \mathbf{W}_i{}^i\mathbf{r}_{i+1} \tag{2}$$

where $\mathbf{W}_i$ is the global transformation matrix from $(\widehat{X}_0, \widehat{Y}_0)$ to (X_i, Y_i), which obeys to the recursive equation

$$\mathbf{W}_i = \mathbf{W}_{i-1}\mathbf{E}_{i-1}\mathbf{A}_i = \widehat{\mathbf{W}}_{i-1}\mathbf{A}_i, \qquad \widehat{\mathbf{W}}_0 = \mathbf{I}. \tag{3}$$

On the basis of the above equations, the kinematics of any point along the arm is fully characterized. For later use in the arm's kinetic energy, also the differential kinematics is needed. In particular, the (scalar) absolute angular velocity of frame (X_i, Y_i) is

$$\dot{\alpha}_i = \sum_{j=1}^{i} \dot{\theta}_j + \sum_{k=1}^{i-1} \dot{y}'_{ke} \tag{4}$$

where the upper dot denotes time derivative. Moreover, the absolute linear velocity of an arm point is

$$\dot{\mathbf{p}}_i = \dot{\mathbf{r}}_i + \dot{\mathbf{W}}_i{}^i\mathbf{p}_i + \mathbf{W}_i{}^i\dot{\mathbf{p}}_i \tag{5}$$

and ${}^i\dot{\mathbf{r}}_{i+1} = {}^i\dot{\mathbf{p}}_i(\ell_i)$. Since the links are assumed inextensible ($\dot{x}_i = 0$), then ${}^i\dot{\mathbf{p}}_i(x_i) = (\,0 \quad \dot{y}_i(x_i)\,)^T$. The computation of (5) takes advantage of the recursions

$$\dot{\mathbf{W}}_i = \dot{\widehat{\mathbf{W}}}_{i-1}\mathbf{A}_i + \widehat{\mathbf{W}}_{i-1}\dot{\mathbf{A}}_i, \qquad \dot{\widehat{\mathbf{W}}}_i = \dot{\mathbf{W}}_i\mathbf{E}_i + \mathbf{W}_i\dot{\mathbf{E}}_i. \tag{6}$$

Also, note that

$$\dot{\mathbf{A}}_i = \mathbf{S}\mathbf{A}_i\dot{\theta}_i, \qquad \dot{\mathbf{E}}_i = \mathbf{S}\dot{y}'_{ie}, \qquad \mathbf{S} = \begin{bmatrix} 0 & -1 \\ 1 & 0 \end{bmatrix}. \tag{7}$$

3. LAGRANGIAN MODELLING

The dynamic equations of motion of a planar n-link flexible arm can be derived following the standard Lagrangian approach, i.e. compute the kinetic energy T and the potential energy U of the system and then form the Lagrangian $L = T - U$ which satisfies the Euler-Lagrange equations

$$\frac{d}{dt}\frac{\partial L}{\partial \dot{q}_i} - \frac{\partial L}{\partial q_i} = f_i, \qquad i = 1, \ldots, N \tag{8}$$

where $\{q_i\}$ are a suitable set of generalized coordinates to be determined, and $\{f_i\}$ are the associated generalized forces acting on the system. The flexibility is thus expressed in terms of $N - n$ variables.

The total kinetic energy is given by the sum of the following contributions:

$$T = \sum_{i=1}^{n} T_{hi} + \sum_{i=1}^{n} T_{\ell i} + T_p. \tag{9}$$

The kinetic energy of the rigid body located at hub i of mass m_{hi} and moment of inertia J_{hi} is

$$T_{hi} = \frac{1}{2} m_{hi} \dot{\mathbf{r}}_i^T \dot{\mathbf{r}}_i + \frac{1}{2} J_{hi} \dot{\alpha}_i^2 \tag{10}$$

with $\dot{\alpha}_i$ as in (4); the kinetic energy pertaining to link i of linear density ρ_i is

$$T_{\ell i} = \frac{1}{2} \int_0^{\ell_i} \rho_i(x_i) \dot{\mathbf{p}}_i^T(x_i) \dot{\mathbf{p}}_i(x_i) dx_i; \tag{11}$$

and the kinetic energy associated to a payload of mass m_p and moment of inertia J_p located at the end of link n is

$$T_p = \frac{1}{2} m_p \dot{\mathbf{r}}_{n+1}^T \dot{\mathbf{r}}_{n+1} + \frac{1}{2} J_p (\dot{\alpha}_n + \dot{y}'_{ne})^2. \tag{12}$$

Remarkably, the evaluation of the expressions in (10–12) exploits the following relations: $\mathbf{A}_i^T \mathbf{A}_i = \mathbf{E}_i^T \mathbf{E}_i = \mathbf{S}^T \mathbf{S} = \mathbf{I}$; $\mathbf{A}_i^T \dot{\mathbf{A}}_i = \mathbf{S} \dot{\theta}_i$; $\mathbf{E}_i^T \dot{\mathbf{E}}_i = (\mathbf{I} y'_{ie} + \mathbf{S}) \dot{y}'_{ie}$.

In absence of gravity (horizontal plane motion), the potential energy is given by

$$U = \sum_{i=1}^{n} U_i = \sum_{i=1}^{n} \frac{1}{2} \int_0^{\ell_i} EI_i(x_i) \left[\frac{d^2 y_i(x_i)}{dx_i^2} \right]^2 dx_i \tag{13}$$

where U_i is the elastic energy stored in link i, being EI_i its flexural rigidity.

4. ASSUMED MODE SHAPES

Links are modelled as Euler-Bernoulli beams of uniform density, i.e. (dropping link subscripts)

$$EI \frac{\partial^4 y(x,t)}{\partial x^4} + \rho \frac{\partial^2 y(x,t)}{\partial t^2} = 0 \tag{14}$$

with *clamped-mass* boundary conditions:

$$y(0,t) = 0, \qquad y'(0,t) = 0 \tag{15a}$$

$$EI \frac{\partial^2 y(x,t)}{\partial x^2}\bigg|_{x=\ell} = -J_L \frac{d^2}{dt^2} \left(\frac{\partial y(x,t)}{\partial x}\bigg|_{x=\ell} \right), \qquad EI \frac{\partial^3 y(x,t)}{\partial x^3}\bigg|_{x=\ell} = M_L \frac{d^2}{dt^2} (y(x,t)|_{x=\ell}) \tag{15b}$$

where M_L and J_L are the actual mass and moment of inertia seen at the link end-point.

In force of space and time separability of solutions to (14–15), a finite-dimensional model (of order m_i) of link flexibility is obtained by the assumed modes technique [2], i.e.

$$y_i(x_i,t) = \sum_{j=1}^{m_i} \phi_{ij}(x_i) \delta_{ij}(t) \tag{16}$$

where $\delta_{ij}(t)$ are the time-varying variables associated with the mode shapes ϕ_{ij} of link i of the form

$$\phi_{ij}(x_i) = C_{1,ij}\sin(\beta_{ij}x_i) + C_{2,ij}\cos(\beta_{ij}x_i) + C_{3,ij}\sinh(\beta_{ij}x_i) + C_{4,ij}\cosh(\beta_{ij}x_i) \quad (17)$$

with $\beta_{ij}^4 = \omega_{ij}^2\rho_i/EI_i$; ω_{ij} are the natural angular frequencies of the related eigenvalue problem for link i. The expressions of the coefficients C in (17) for a single link can be found in [11]. However, it must be pointed out that in the multi-link case M_L and J_L for the intermediate links are time-varying quantities depending on the actual arm configuration.

5. CLOSED-FORM EQUATIONS OF MOTION

On the basis of the above analysis, the closed-form equations of motion for a planar n-link flexible arm can be written as

$$\mathbf{B}(\mathbf{q})\ddot{\mathbf{q}} + \mathbf{h}(\mathbf{q},\dot{\mathbf{q}}) + \mathbf{D}(\mathbf{q},\dot{\mathbf{q}})\dot{\mathbf{q}} + \mathbf{K}(\mathbf{q})\mathbf{q} = \mathbf{Q}(\mathbf{q})\mathbf{u} \quad (18)$$

where $\mathbf{q} = (\,\theta_1 \ldots \theta_n\delta_{11} \ldots \delta_{1,m_1} \ \ldots \ \delta_{n,1} \ldots \delta_{n,m_n}\,)^T$ is the N-vector of generalized coordinates ($N = n + \sum m_i$), and $\mathbf{u}$ is the n-vector of joint (actuator) torques. $\mathbf{B}$ is the positive-definite symmetric inertia matrix, $\mathbf{h}$ is the vector of Coriolis and centrifugal forces, $\mathbf{D}$ is an additional structural damping diagonal matrix, $\mathbf{K}$ is the stiffness diagonal matrix ($K_1 = \ldots = K_n = 0; K_{n+1}, \ldots, K_N > 0$), $\mathbf{Q}$ is the input weighting matrix of the form $(\,\mathbf{I} \quad \mathbf{O}^T\,)^T$ due to the clamped link assumptions.

If a complete ortho-normalization of the mode shapes is performed, convenient simplifications arise in the diagonal blocks of the inertia matrix relative to the deflections of each link. Also, the stiffness coefficients take on the values $\omega_{ij}^2 m_i$, being m_i the mass of link i.

Recall that the components of $\mathbf{h}$ can be evaluated through the Christoffel symbols, i.e.

$$h_i = \sum_{j=1}^{N}\sum_{k=1}^{N}\left(\frac{\partial B_{ij}}{\partial q_k} - \frac{1}{2}\frac{\partial B_{jk}}{\partial q_i}\right)\dot{q}_j\dot{q}_k. \quad (19)$$

In the remainder, the terms in equation (18) are customized to a specific structure, namely the two-link arm in Fig. 1 with two modes of deflection for each link. The resulting model is casted in a computationally advantageous form, where a set of constant parameters appear that depend on the mechanical properties of the arm. The inertia matrix turns out of the form:†

$$B_{11} = b_{111} + b_{112}c_2 + (b_{113}t_1 + b_{114}t_2)s_2$$
$$B_{12} = b_{121} + b_{122}c_2 + (b_{123}t_1 + b_{124}t_2)s_2$$
$$B_{13} = b_{131} + b_{132}c_2 + (b_{133}t_2 + b_{134}\delta_{12})s_2$$
$$B_{14} = b_{141} + b_{142}c_2 + (b_{143}t_2 + b_{144}\delta_{11})s_2$$
$$B_{15} = b_{151} + b_{152}c_2 + b_{153}t_1s_2$$
$$B_{16} = b_{161} + b_{162}c_2 + b_{163}t_1s_2$$
$$B_{22} = b_{221}$$
$$B_{23} = b_{231} + b_{232}c_2 + (b_{233}t_2 + b_{234}t_3)s_2$$
$$B_{24} = b_{241} + b_{242}c_2 + (b_{243}t_2 + b_{244}t_3)s_2$$
$$B_{25} = b_{251}$$
$$B_{26} = b_{261}$$
$$B_{33} = b_{331} + b_{332}c_2 + b_{333}t_2s_2$$
$$B_{34} = b_{341} + b_{342}c_2 + b_{343}t_2s_2$$
$$B_{35} = b_{351} + b_{352}c_2 + b_{353}t_3s_2$$
$$B_{36} = b_{361} + b_{362}c_2 + b_{363}t_3s_2$$
$$B_{44} = b_{441} + b_{442}c_2 + b_{443}t_2s_2$$
$$B_{45} = b_{451} + b_{452}c_2 + b_{453}t_3s_2$$
$$B_{46} = b_{461} + b_{462}c_2 + b_{463}t_3s_2$$
$$B_{55} = b_{551}$$
$$B_{56} = b_{561}$$
$$B_{66} = b_{661}$$

† Due to lack of space, the coefficients' expressions are not given but can be obtained from the Authors.

where $s_2 = \sin\theta_2$, $c_2 = \cos\theta_2$, and

$$t_1 = t_{11}\delta_{11} + t_{12}\delta_{12}, \qquad t_2 = t_{21}\delta_{21} + t_{22}\delta_{22}, \qquad t_3 = t_{31}\delta_{11} + t_{32}\delta_{12}.$$

Analogous format results for the nonlinear terms in **h** computed via (19).

Concerning the boundary conditions (15*b*), it is obviously $M_{L2} = m_p$ and $J_{L2} = J_p$ which implies $b_{551} = b_{661} = m_2$ and $b_{561} = 0$. On the other hand, the approximate choice $M_{L1} = m_{h2} + m_2 + m_p$ and $J_{L1} = J_{h2} + J_{o2} + J_p + m_p\ell_2^2$ (J_{oi} is link i inertia reported at joint i) is made which implies $b_{331} = b_{441} = m_1$ and $b_{341} = 0$, thus leaving non-zero time-varying terms in B_{33}, B_{44}, and B_{34}.

6. SIMULATION RESULTS

In order to test the dynamic model obtained for the two-link arm, a set of simulations has been performed. The physical parameters of the arm with uniform mass density are: $\ell_1 = \ell_2 = 0.50$ m, $m_1 = m_2 = m_p = 0.10$ kg, $m_{h2} = 1.0$ kg, $J_{o1} = J_{o2} = 0.0083$ kg-m^2, $J_{h1} = J_{h2} = 0.10$ kg-m^2, $J_p = 0.00050$ kg-m^2, $EI_1 = EI_2 = 1.0$ N-m^2.

The computed natural frequencies are 0.48, 1.8 Hz for link 1, and 2.2, 16 Hz for link 2. The resulting mode shapes are plotted in Fig. 2, where one can see that, compared to the clamped-free case, ϕ_{12} does not present the usual node at $x_2 > 0$.

Figs. 3–4 show the dependence of the internal vibrations of the arm on the joint configuration when an initial deformation is forced into the system. In particular, when $\theta_2(0) = 0$ the vibrations coupling between the two links is strong; instead, when $\theta_2(0) = \pi/2$ the second link is hardly affected by an initial deformation of the first link (note the two orders of magnitude difference on δ_{2j}).

Next, a 2 sec symmetric bang-bang input torque of 0.2 N-m has been applied at both joints. The induced vibrations are shown in Fig. 5, while the resulting joint and tip motions are reported in Fig. 6. Finally, Figs. 7–8 give evidence of the improvement in the arm motion when structural damping is added ($D_i = 0.1\sqrt{K_i}$).

7. CONCLUSIONS

This paper has presented the derivation of the closed-form equations of motion for a planar multi-link flexible arm, following a Lagrangian/assumed modes technique. The model has been customized for a two-link arm in order to develop a case study where the effects of rigid and flexible dynamics interaction are evident. Further research will be devoted to studying the implications of using time-varying boundary conditions and to designing model-based control algorithms for trajectory tracking.

REFERENCES

[1] W.J. Book, "Recursive Lagrangian dynamics of flexible manipulator arms," *Int. J. Rob. Res.*, Vol. 3, No. 3, pp. 87–101, 1984.

[2] L. Meirovitch, *Analytical Methods in Vibrations*, Macmillan, New York, 1967.

[3] R.H. Cannon, Jr. and E. Schmitz, "Initial experiments on the end-point control of a flexible one-link robot," *Int. J. Rob. Res.*, Vol. 3, No. 3, pp. 62–75, 1984.

[4] E. Bayo, "A finite element approach to control the end-point motion of a single-link flexible robot," *J. Rob. Syst.*, Vol. 4, pp. 63–75, 1987.

[5] P. Tomei and A. Tornambè, "Approximate modeling of robots having elastic links," *IEEE Trans. Syst., Man, Cybern.*, Vol. 18, pp. 831–840, 1988.

[6] G.G. Hastings and W.J. Book, "A linear dynamic model for flexible robotic manipulators," *IEEE Contr. Syst. Mag.*, Vol. 7, No. 1, pp. 61–64, 1987.

[7] F. Bellezza, L. Lanari, and G. Ulivi, "Exact modeling of the slewing flexible link," submitted to *1990 IEEE Int. Conf. Rob., Autom.*, Cincinnati, OH.

[8] S. Cetinkunt, B. Siciliano, and W.J. Book, "Symbolic modelling and dynamic analysis of flexible manipulators," *Proc. 1986 IEEE Int. Conf. Syst., Man, Cybern.*, Atlanta, GA, pp. 798–803.

[9] C.M. Oakley and R.H. Cannon, Jr., "Initial experiments on the control of a two-link manipulator with a very flexible forearm," *Proc. 1988 Amer. Contr. Conf.*, Atlanta, GA, pp. 996–1002.

[10] E. Schmitz, "Modeling and control of a planar manipulator with an elastic forearm," *Proc. 1989 IEEE Int. Conf. Rob., Autom.*, Scottsdale, AZ, pp. 267–278.

[11] A. De Luca and B. Siciliano, "Trajectory control of a nonlinear one-link flexible arm," *Int. J. Contr.*, to appear, 1989.

This paper is based on work supported by the *Ministero dell'Università e della Ricerca Scientifica e Tecnologica* under 40% and 60% funds.

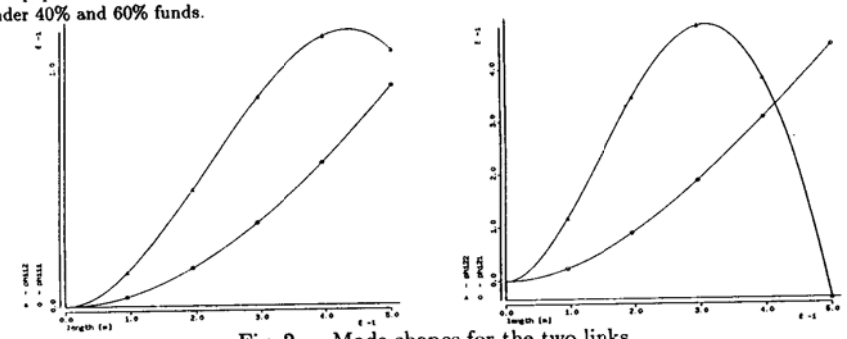

Fig. 2 — Mode shapes for the two links

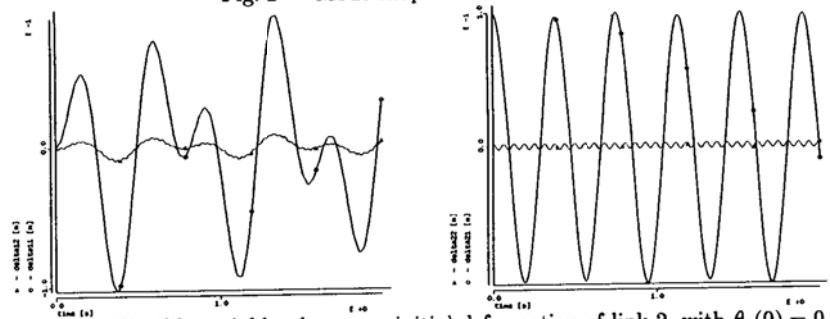

Fig. 3 — Flexible variables due to an initial deformation of link 2, with $\theta_2(0) = 0$

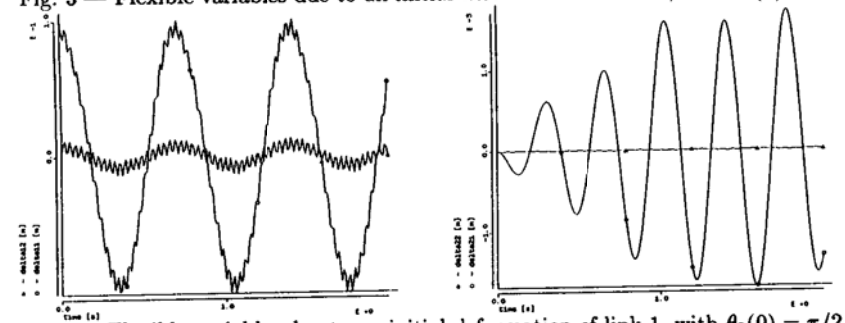

Fig. 4 — Flexible variables due to an initial deformation of link 1, with $\theta_2(0) = \pi/2$

View publication stats

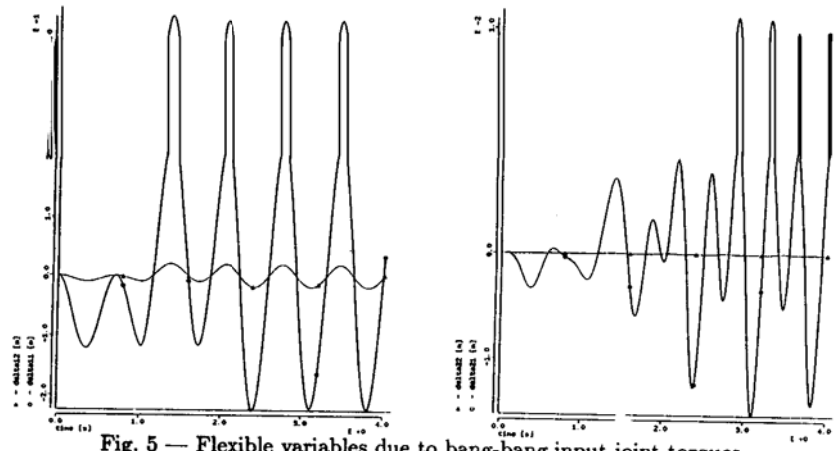

Fig. 5 — Flexible variables due to bang-bang input joint torques

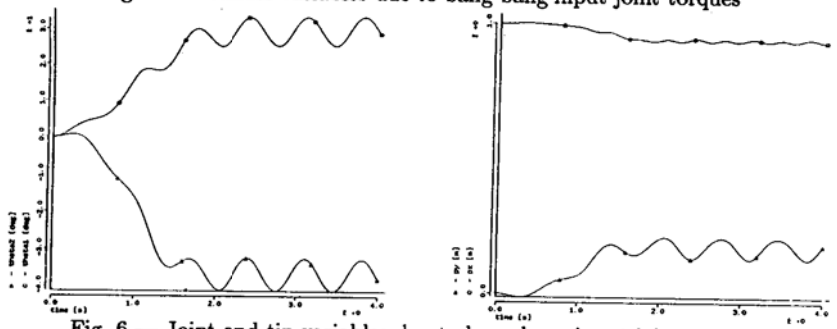

Fig. 6 — Joint and tip variables due to bang-bang input joint torques

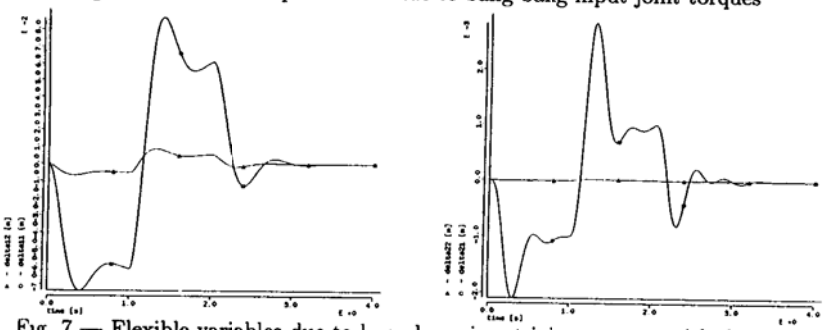

Fig. 7 — Flexible variables due to bang-bang input joint torques, with damping

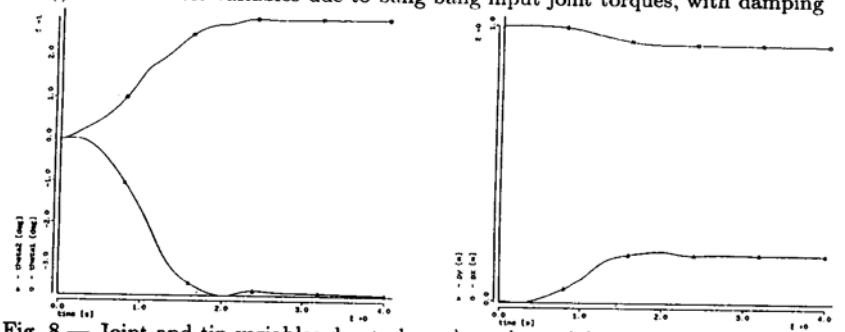

Fig. 8 — Joint and tip variables due to bang-bang input joint torques, with damping